Neuron
Article

Neuroprotection through Excitability and mTOR Required in ALS Motoneurons to Delay Disease and Extend Survival

Smita Saxena,[1,2,6] Francesco Roselli,[1,6] Katyayani Singh,[2] Kerstin Leptien,[1] Jean-Pierre Julien,[5] Francois Gros-Louis,[3,4] and Pico Caroni[1,*]
[1]Friedrich Miescher Institut, Maulbeerstrasse 66, CH-4058 Basel, Switzerland
[2]Institute of Cell Biology, University of Bern, Balzerstrasse 4, CH-3012 Bern, Switzerland
[3]Centre LOEX, CHU de Quebec Research Center
[4]Department of Surgery, Faculty of Medicine
[5]Department of Psychiatry and Neuroscience
Laval University, Quebec G1V 0A6, Canada
[6]These authors contributed equally to this work
*Correspondence: caroni@fmi.ch
http://dx.doi.org/10.1016/j.neuron.2013.07.027

SUMMARY

Delaying clinical disease onset would greatly reduce neurodegenerative disease burden, but the mechanisms influencing early preclinical progression are poorly understood. Here, we show that in mouse models of familial motoneuron (MN) disease, SOD1 mutants specifically render vulnerable MNs dependent on endogenous neuroprotection signaling involving excitability and mammalian target of rapamycin (mTOR). The most vulnerable low-excitability FF MNs already exhibited evidence of pathology and endogenous neuroprotection recruitment early postnatally. Enhancing MN excitability promoted MN neuroprotection and reversed misfolded SOD1 (misfSOD1) accumulation and MN pathology, whereas reducing MN excitability augmented misfSOD1 accumulation and accelerated disease. Inhibiting metabotropic cholinergic signaling onto MNs reduced ER stress, but enhanced misfSOD1 accumulation and prevented mTOR activation in alpha-MNs. Modulating excitability and/or alpha-MN mTOR activity had comparable effects on the progression rates of motor dysfunction, denervation, and death. Therefore, excitability and mTOR are key endogenous neuroprotection mechanisms in motoneurons to counteract clinically important disease progression in ALS.

INTRODUCTION

Neurodegenerative diseases can involve decades-long preclinical phases of subtle pathologies (e.g., Reiman et al., 2004; Kok et al., 2009) followed by relentlessly progressing neurodegeneration. Any intervention that could delay clinical disease onset would have dramatic consequences on the burden of disease, but the mechanisms that influence early progression processes are poorly understood (Palop and Mucke, 2010; Saxena and Caroni, 2011). The study of early disease mechanisms in vivo has been greatly aided by the availability of experimentally tractable animal models in which disease-related processes unfold according to specific cellular patterns and predictable temporal schedules. Nevertheless, dissecting disease-relevant causality relationships has remained challenging, mainly due to the difficulties inherent in discriminating underlying causes from adaptive consequences and harmless epiphenomena during slowly progressing early phases of disease in vivo. Because disease-related deficits might be neutralized initially through homeostatic and compensatory processes, we hypothesize that adaptive responses are likely to be predominant during early phases of disease. Accordingly, the identification and investigation of disease-relevant early dysfunction might benefit from a focus on candidate endogenous neuroprotection mechanisms that might compensate for mounting disease-related cellular malfunctions. Taking such an approach here, we focused on the early vulnerability of low-excitability fast-fatigable (FF) motoneurons (MNs) in amyotrophic lateral sclerosis (ALS) (Pun et al., 2006; Saxena et al., 2009; Kanning et al., 2010) and investigated how excitability might relate to the early progression of pathology and dysfunctions in mouse models of familial ALS. We provide evidence that excitability and mammalian target of Rapamycin (mTOR) together provide endogenous neuroprotection to familial amyotrophic lateral sclerosis (FALS) alpha-MNs and that a growing deficit in excitability-related signaling drives pathology and dysfunction in superoxide dismutase 1 (SOD1) mouse models of FALS.

Transgenic mice overexpressing FALS-associated human mutant SOD1 (mutSOD1) under the control of a human SOD1 promoter cassette have provided valuable animal models to investigate mechanisms of disease in ALS (Gurney et al., 1994; Boillée et al., 2006; Kanning et al., 2010; Saxena and Caroni, 2011). The mice exhibit characteristic MN disease features, including long presymptomatic phases of increasing cell specific pathology and dysfunction and rapidly progressing clinical phases leading to paralysis and death. MN pathology in

SOD1-based FALS and in the corresponding rodent models closely resembles sporadic cases of ALS (Boillée et al., 2006; Kanning et al., 2010), establishing mutant mice as valid genetic models to investigate early mechanisms of disease in neurodegeneration. Notably, spinal alpha-MN pathology and dysfunction develops in the mice with remarkable temporal reproducibility, allowing the combination of data from individual mutant mice of different ages into virtual longitudinal studies (Pun et al., 2006; Saxena et al., 2009). These studies have provided evidence that in SOD1-based FALS models, low-excitability FF MNs innervating hind limb muscles abruptly prune their peripheral axonal arborizations within about 2 days (Pun et al., 2006). Medium-excitability fatigue-resistant (FR) MNs disconnect from the periphery ~30 days later, whereas highly excitable slow (S) MNs are resistant and only partially disconnect from target muscles when mice reach end-stage paralytic disease (Pun et al., 2006). In each alpha-MN subpopulation, the selective denervation processes are preceded first by gradually increasing endoplasmic reticulum (ER) stress, followed by an unfolded protein response ~20 days before denervation (Saxena et al., 2009), and by axonal pathology during the last 2 weeks before denervation (Pun et al., 2006). Taken together, these findings provided evidence for a higher vulnerability of low-excitability FF MNs and a relatively higher resistance of high-excitability S MNs in FALS mice. Available clinical data are consistent with the notion that disease progression in ALS patients involves comparable differential vulnerabilities of low- and high-excitability alpha-MNs (Kanning et al., 2010). Whether the low excitability of FF MNs might account for their higher vulnerability to degeneration has, however, remained unclear.

Early alterations in excitability have been reported in sporadic and familial ALS, as well as in mouse models of FALS (Bories et al., 2007; Vucic et al., 2008; Saxena and Caroni, 2011). Reduced levels of astrocytic glutamate transporter and enhanced excitability have led to the hypothesis that excessive excitability and excitotoxicity might be major pathogenic factors in ALS (Rothstein, 1995-1996; Van Den Bosch et al., 2006). On the other hand, studies of cultured spinal MNs have revealed a specific pathway affecting ~50% of mutant MNs and to which wild-type MNs and mutant non-MNs are immune (Raoul et al., 2002; Kanning et al., 2010). Those results have implicated excess MN cytosolic calcium and ER stress in FasL- and nitric oxide-induced cell death upon downregulation of the ER calcium sensor and chaperon Calreticulin in FALS MNs (Bernard-Marissal et al., 2012). Calreticulin (Molinari et al., 2004) did not protect wild-type MNs from activation of the FasL pathway, suggesting that the vulnerability of alpha-MNs induced by mutSOD1 might specifically involve calcium and ER pathways (Bernard-Marissal et al., 2012). Reduced Calreticulin levels were mainly detected in vulnerable FF MNs of tibialis anterior, but not in resistant MNs of soleus in presymptomatic SOD1(G93A) mice, suggesting that the specific calcium-related toxicity pathway also operates in FALS MNs in vivo (Bernard-Marissal et al., 2012). The enhanced cytosolic calcium levels might reduce the excitability of MNs through the activation of calcium-dependent hyperpolarizing conductances (Miles et al., 2007). Accordingly, MN excitability signaling in ALS might primarily be reduced, not enhanced. Furthermore, whereas ER stress in FALS (Kanekura et al., 2009; Saxena and Caroni, 2011) might be due to the accumulation of misfolded proteins, alternative scenarios (e.g., including a depletion of lumenal calcium in the ER) are also possible (Tu et al., 2006; Wang and Kaufman, 2012). Taken together, these considerations have suggested contrasting potential scenarios of how alterations in excitability and ER stress might influence early phases of disease in ALS, but whether and how any of these have a role in disease progression has remained unclear.

Here, we investigated a possible role of excitability in disease progression in presymptomatic FALS mice. We first established antibodies against misfolded SOD1 (misfSOD1) (Gros-Louis et al., 2010) as specific and sensitive cellular reagents to detect disease-relevant pathology in early presymptomatic FALS mice. We then provided evidence that disease-associated SOD1 mutants specifically render alpha-MNs dependent on endogenous neuroprotection signaling involving excitability and mTOR. During a protracted presymptomatic phase, inhibiting MN excitability was sufficient to induce comparable pathology and enhanced compensatory responses in all vulnerable alpha-MNs, suggesting that the relatively higher resilience of FR and S alpha-MNs to disease is related to their comparatively higher excitabilities. Enhancing MN excitability augmented neuroprotection pathways in FALS MNs. Modulating excitability or alpha-MN mTOR influenced the progression rates of motor dysfunction, muscle denervation, and death, providing evidence that excitability and mTOR are key endogenous neuroprotection mechanisms to counteract clinically important disease progression in FALS. Taken together, our results identify critical early dysfunction processes in FALS MNs, providing support to the notion that a focus on endogenous neuroprotection pathways in presymptomatic mice provides a valuable approach to unravel causal relationships between early disease-related dysfunctions and corresponding compensatory responses. Their elucidation might guide the elaboration of early therapeutic strategies in ALS.

RESULTS

Early Disease-Related Misfolded SOD1 Accumulation in Vulnerable MNs

To monitor relevant neuronal dysfunction in presymptomatic FALS mice, we first sought to establish specific early cellular disease-related markers. Because mutant SOD1 causes disease in the transgenic mice, we reasoned that misfSOD1 accumulation might provide an unbiased readout of the disease process. Accordingly, we investigated misfSOD1 immunoreactivity using conformation specific monoclonal antibodies D3H5 or A5C3, which specifically detect disease-associated epitopes of this ubiquitous cytosolic protein (Gros-Louis et al., 2010). Alpha-MNs were identified as ventral horn cells, which were positive for vesicular acetylcholine transporter (VAChT) or choline acetyl transferase (ChAT) immunoreactivity, and were surrounded by brightly labeled VAChT-positive C-boutons, the presynaptic endings of cholinergic partition cells (Miles et al., 2007; Zagoraiou et al., 2009). Most of the experiments were carried out in transgenic mice overexpressing moderate (*TgG93Aslow*; abbreviated as *G93A-s*) or high (*TgG93Afast*; abbreviated as *G93A-f*) levels of human SOD1(G93A) under the control of a human SOD1 minigene, but qualitatively comparable results were

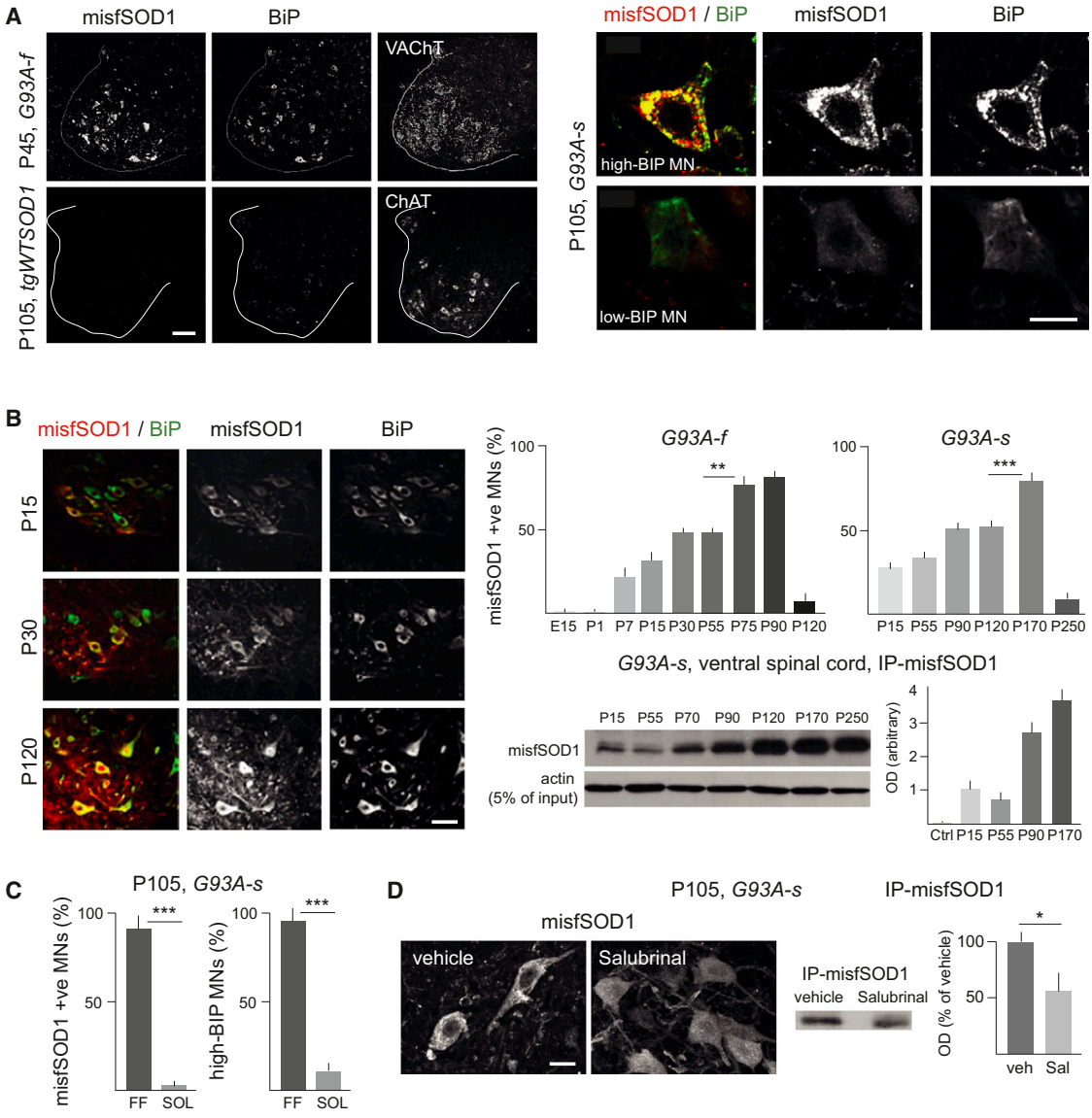

Figure 1. Early Disease-Related Misfolded SOD1 Accumulation in Vulnerable MNs

(A) MisfSOD1 accumulation specifically in FALS MNs exhibiting high ER stress. Left: codistribution of misfSOD1 and BiP signals in FALS MNs and absence of detectable signals in transgenic mice overexpressing wild-type human SOD1. Right: accumulation of misfSOD1 specifically in FALS MNs with high BiP signals. Scale bars represent 100 μm (left), 25 μm (right).

(B) Age dependence of misfSOD1 accumulation in FALS MNs. IP-western: immunoprecipitation with misfSOD1 antibody and immunoblot with pan-SOD1 antibody. Quantitative analysis, misfSOD1-positive (+ve); MNs, percentage of VAChT-positive lumbar spinal cord ventral horn cells with detectable misfSOD1 accumulation; N = 3–5 mice each; error bars represent SEM. *p < 0.05, **p < 0.01 ***p < 0.001 in post-ANOVA Tukey test (same for all figures); OD, optical density for misfSOD1 signal (N = 3 mice each; bars represent SEM). Scale bar represents 50 μm.

(C) Accumulation of misfSOD1 and BiP signals specifically in most vulnerable FF MNs. Immunocytochemistry signal in back-labeled, rhodamine-dextran positive MNs. N = 3 mice each; error bars represent SEM.

(D) Reduced MN misfSOD1 accumulation in mice treated with ER stress reducing agent Salubrinal (every second day, from P90 to P105). Quantitative analysis: IP-western as in (B); signal in Salubrinal-treated mice expressed as percent of vehicle-treated mice (N = 3 mice; SEM). Scale bar represents 20 μm.

obtained with transgenic mice overexpressing a human SOD1(G85R) mutant.

From postnatal day (P) 7 on, but not yet at P1 (nor at embryonic day 15), we detected a distinct misfSOD1 signal specifically in a subpopulation of alpha-MNs in the lumbar spinal cord in mutant mice (Figures 1A and 1B). No misfSOD1 signals were detected in nontransgenic wild-type mice, or in transgenic mice overexpressing human wild-type SOD1 at any age (*TgwtSOD1* mice; Figure 1A). MN misfSOD1 signals remained confined to 40%–50% of lumbar spinal cord alpha-MNs until P55–60 (*G93A-f*) or P140–150 (*G93A-s*) (Figure 1B). Retrograde labeling experiments involving rhodamine-dextran applied locally to

identified muscle compartments exclusively innervated by FF (lateral gastrocnemius, subcompartment l1), or mixed FR + S MNs (soleus) (Saxena et al., 2009) revealed that during this early presymptomatic phase, misfSOD1 specifically accumulated in FF MNs (Figure 1C). Consistent with the notion that misfolded mutant protein accumulation was initially specifically confined to the most vulnerable FF MNs, the distribution of the misfSOD1 signal among MNs closely resembled that of the ER chaperon binding immunoglobulin protein (BiP) (Figure 1C), which specifically accumulates in FF MNs in presymptomatic mice (Saxena et al., 2009). Indeed, one of the antigens (A5C3) highlighted misfSOD1 accumulation closely codistributed with ER (Figure 1A), whereas D3H5 yielded more intense labeling signals that were distributed throughout the cytosol of MNs. After this protracted presymptomatic stage, and 5–10 days before an unfolded protein response (UPR) in FR MNs, the fraction of lumbar spinal cord alpha-MNs positive for misfSOD1 increased to >80% of total, thus including FR MNs (Figure 1B). Consistent with a specific disease association, MN misfSOD1 immunoreactivity signals and ventral spinal cord immunoprecipitation (IP)-western levels were reduced in early presymptomatic mutant mice (*G93A-s*, P105; i.e., in FF MNs) treated with the anti-ER stress reagent Salubrinal, which delays disease progression (Figure 1D; Saxena et al., 2009). The Salubrinal treatment also abolished the codistribution of A5C3 antigen with ER (not shown). We concluded that in the FALS disease models MN pathology as revealed by misfSOD1 accumulation is already detectable specifically in FF MNs at 1 week of age (but not before) and becomes detectable in FR MN shortly before the onset of the clinical phase.

Within a FALS Context alpha-MNs Depend on Excitability to Prevent Pathology

To investigate early mechanisms of disease in FALS, we then determined whether the higher relative vulnerability of FF MNs might be related to their lower excitability and whether reducing excitability might selectively compromise FALS alpha-MNs. In a first set of experiments, we treated FALS mice with nonparalyzing doses of the α-amino-3-hydroxy-5-methyl-4-isoxazolepropionic acid (AMPA) receptor antagonist 6-cyano-7-nitroquinoxaline-2,3-dione (CNQX) and analyzed misfSOD1 accumulation patterns in mutant mice that had been exposed to CNQX during 1, 3, 5, or 20 days. Up to 5 days of treatments had no detectable effects in a grid test assay that measured muscle strength in wild-type or FALS mice, indicating that at these doses CNQX did not majorly affect MN firing activities (not shown). Nevertheless, the CNQX treatments had a dramatic impact on misfSOD1 accumulation and ER stress in alpha-MNs. In early presymptomatic mutant mice treated with CNQX for 1–3 days, misfSOD1 accumulation increased strongly in MNs, where it spread to most lumbar spinal alpha-MNs (Figure 2A). In parallel, alpha-MNs exhibited massively elevated levels of ER chaperon BiP and of the UPR marker Pi-eIF2a (Figures 2A; Figure S1 available online). By contrast, the same treatments did not detectably enhance misfSOD1, BiP, or Pi-eIF2a levels in non-MNs in the spinal cord, or in other parts of the brain of SOD1 mutant mice (Figure S1; not shown). Supporting the notion that reduced excitability augments MN pathology in mutant SOD1 mice, administration of the serotonin antagonists Ketanserin + Way ($5\text{-HT}_{1A/2A}$) also rapidly augmented misfSOD1 accumulation and ER stress in alpha-MNs (Figure 2A). N-methyl-D-aspartate (NMDA) receptor inhibition with AP5 was as effective as CNQX in augmenting alpha-MN misfSOD1 and ER stress, suggesting that the dramatic increase in pathology specifically in alpha-MN was due to reduced excitability-related signaling (Figure 2A). Unlike short-term treatments during 1–5 days, prolonged treatments with CNQX during 20 days induced accumulation of misfSOD1 and BiP in a majority of neurons in the spinal cord and in the rest of the CNS in SOD1 mutant mice (Figure S1). Even a prolonged attenuation of AMPA receptor transmission however failed to induce signs of UPR outside alpha-MNs (Figure S1).

To determine whether alpha-MNs might be most affected by reduced excitability specifically in a disease context, we delivered CNQX to *TgwtSOD1* mice that ubiquitously overexpress high levels of wild-type human SOD1 and only develop mild MN pathology late in life (Figure S1). Up to five days of CNQX did not induce any detectable ER stress or accumulation of misfSOD1 in *TgwtSOD1* alpha-MNs (Figure S1). Twenty days of CNQX did induce a robust and closely comparable accumulation of BiP immunoreactivity in spinal MNs and non-MNs but only induced misfSOD1 accumulation and ER stress in few MNs in the *TgwtSOD1* mice (Figure S1). A 20 day regime of CNQX in nontransgenic wild-type mice again induced closely comparable accumulations of BiP in spinal MNs and non-MNs, albeit at lower levels than in *TgwtSOD1* mice (Figure S1). These results suggested that although chronic reduction of excitability during 20 days induces comparable ER stress in all neurons and in all genetic backgrounds, disease-related mutSOD1 greatly and specifically sensitizes alpha-MNs to adverse effects of reduced excitability.

To determine whether FALS neurons might be specifically sensitized to reduced excitability as opposed to being generally sensitized to stressors, we induced robust widespread ER stress in early presymptomatic FALS mice by intraperitoneal injections of Tunicamycin or Thapsigargin (Figure 2B). Two days later, drug-treated mice exhibited strongly elevated levels of the ER chaperon BiP in most spinal cord neurons (Figure 2C). By contrast, massively elevated levels of misfSOD1 were specifically induced in alpha-MNs, but were absent in other neurons (Figures 2B and 2C). When *tgwtSOD1* mice were subjected to the same treatment, misfSOD1 accumulation was much less pronounced than in FALS mice, but it was again restricted to alpha-MNs (Figures 2B and 2C). Interestingly, cerebellar Purkinje cells also exhibited selective misfSOD1 accumulation upon enhanced ER stress in FALS and *tgwtSOD1* mice (Figure 2B), but they lacked detectable misfSOD1 signals in FALS mice even upon 5 days of CNQX treatment (not shown, but see Figure S1 for 20 day CNQX treatment). These results revealed that intense ER stress is not sufficient to induce misfSOD1 accumulation in most FALS neurons and provided evidence for the existence of a specific relationship between SOD1-related pathology, excitability and stressors selectively in alpha-MNs (Ezzi et al., 2007; Pokrishevsky et al., 2012).

Excitability Modulates Disease Progression in FALS

To investigate whether enhanced excitability might negatively modulate the accumulation of FALS-related pathology in MNs,

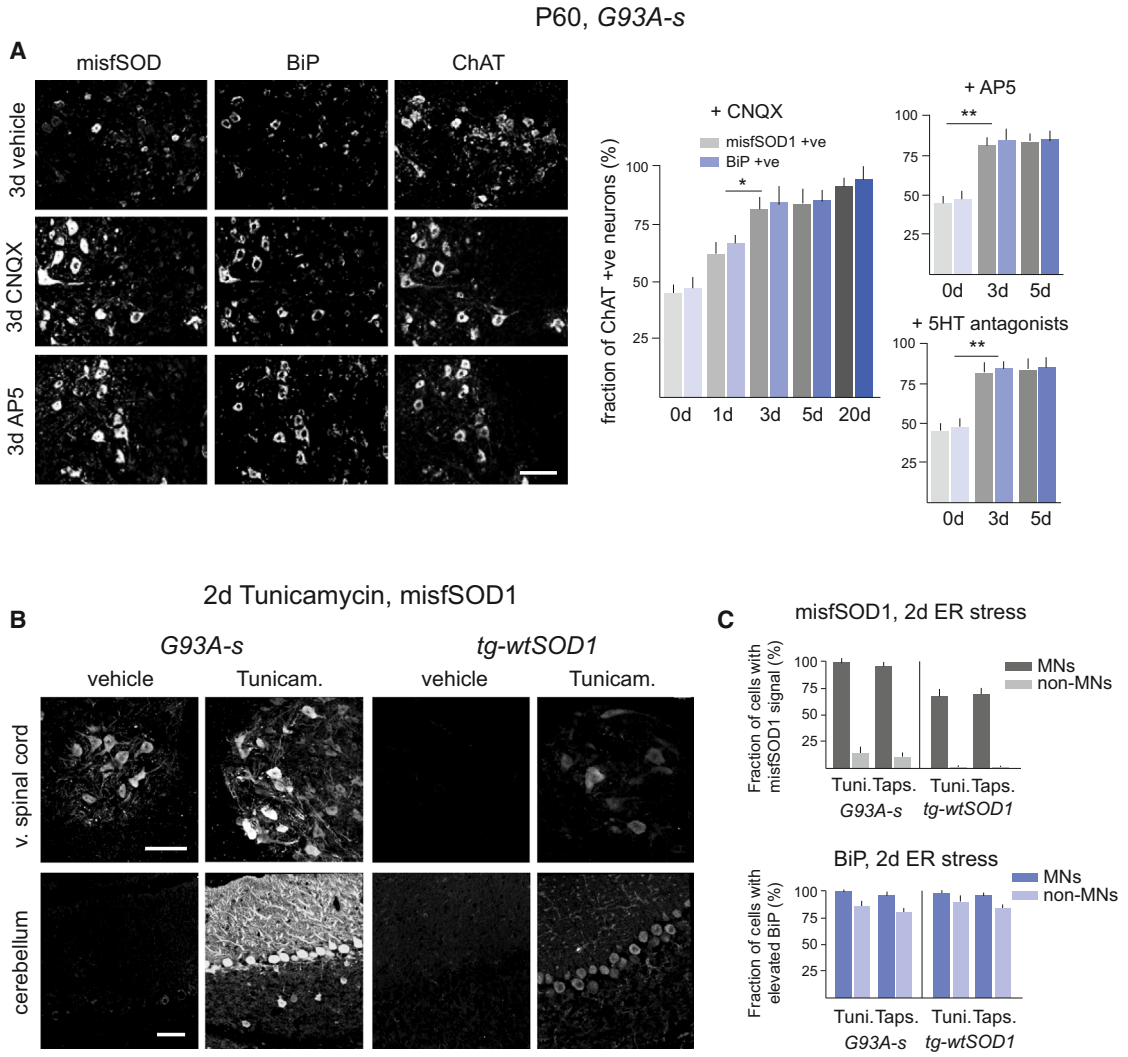

Figure 2. High Vulnerability Specifically of Spinal FALS Alpha-MNs to Reduced Excitability or ER Stress

(A) Short-term treatments with inhibitors of AMPA, NMDA, or 5HT receptors lead to enhanced ER stress and misfSOD1 accumulation in most alpha-MNs of FALS mice. N = 3 mice each; SEM. Scale bar represents 100 μm.

(B and C) Treatment with ER stress inducing agents Tunicamycin or Thapsigargin in transgenic mice overexpressing wild-type or mutant SOD1 induces BiP expression in most neurons but misfSOD1 accumulation specifically in alpha-MNs and cerebellar Purkinje cells (B). Tuni, Tunicamycin; Tapsi, Thapsigargin. Quantitative analysis (C). N = 3 mice each; SEM. Scale bar represents 150 μm (B).

See also Figure S1.

we analyzed mutant SOD1 mice treated with the receptor agonist AMPA. AMPA greatly reduced the accumulation of misfSOD1 in alpha-MNs of presymptomatic and symptomatic mutant SOD1 mice (Figure 3A). Furthermore, AMPA significantly reduced the accumulation of ER stress and UPR markers in presymptomatic mice, albeit not at more advanced phases of disease (Figure 3A). Interestingly, AMPA was comparably effective in reducing misfSOD1 accumulation when drug administration regimes were started at early or late presymptomatic stages (Figure 3A), suggesting that misfSOD1 accumulation in FALS alpha-MNs is a dynamic process, which can be reversed by enhanced excitability. Notably, AMPA counteracted the downregulation of Calreticulin in FF MNs (Figure 3B), the ER chaperon and lumenal calcium sensor, which is a disease-specific trigger of dysfunction and death in selectively vulnerable FALS alpha-MNs (Bernard-Marissal et al., 2012). Taken together, these results provided evidence that although reduced excitability specifically aggravates disease-related pathology in FALS alpha-MNs, enhanced excitability can specifically protect the same vulnerable alpha-MNs.

To investigate whether AMPA promotes neuroprotection pathways in presymptomatic FALS MNs, we monitored accumulation levels of the calcium-dependent neuroprotection proteins GADD45β, DREAM, and Btg2 (Zhang et al., 2009) in wild-type and *G93A-f* mice. MN GADD45β immunoreactivity was elevated in FALS compared to wild-type MNs (Figure 3C).

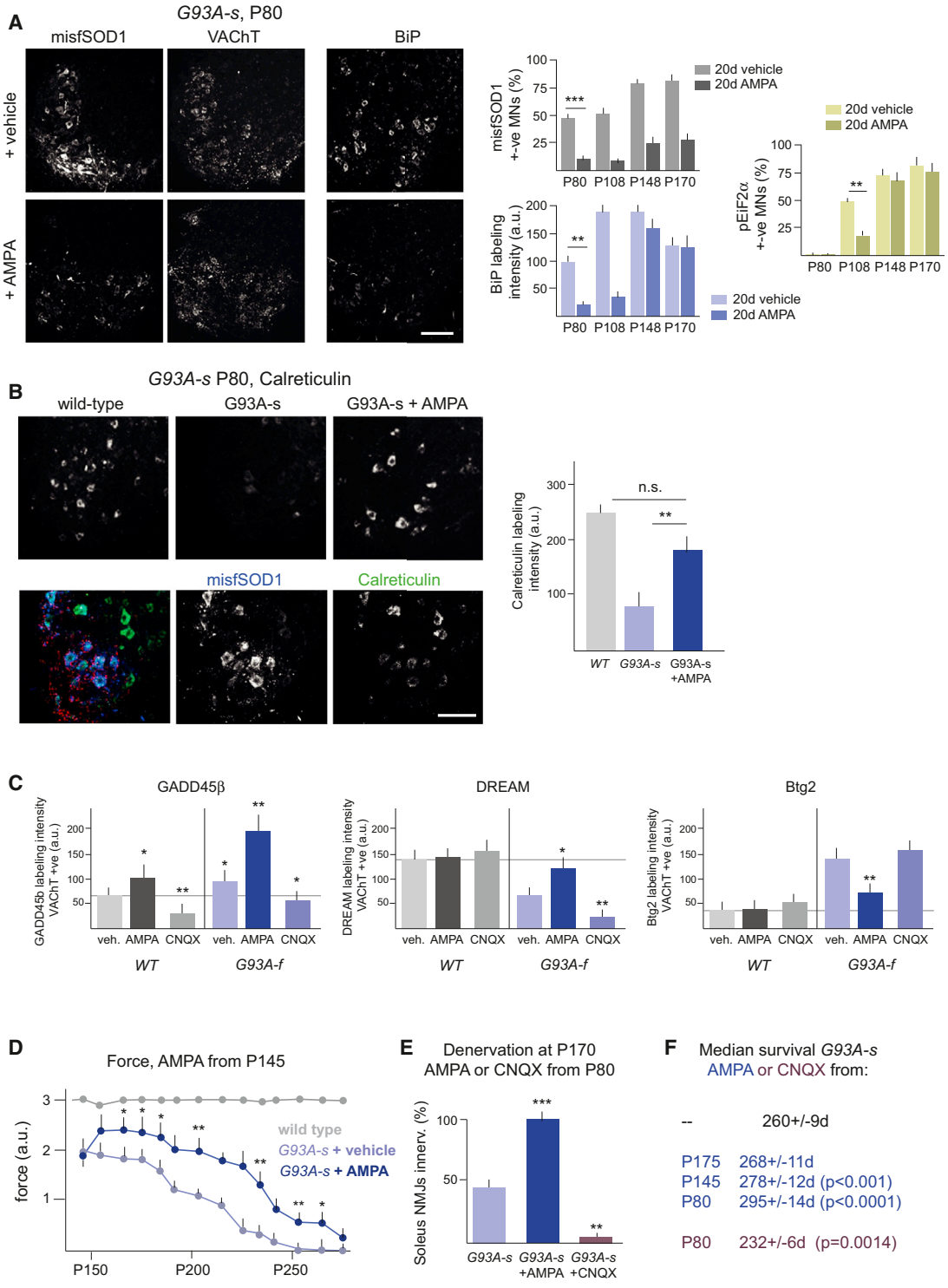

Figure 3. AMPA Receptor Agonist Treatment in FALS Mice Enhances Neuroprotection Pathways in MNs, Protects alpha-MNs against Pathology, and Delays Degeneration and Death

(A) AMPA protects alpha-MNs against pathology in presymptomatic FALS mice. N = 3 mice each; SEM; AMPA every second day for 20 days. Scale bar represents 150 μm.

(B) AMPA prevents downregulation of Calreticulin in alpha-MNs of FALS mice. N = 3 mice each; SEM. Scale bar represents 100 μm.

(C) Activation of neuroprotection pathway in MNs by AMPA and inhibition by CNQX. N = 6 mice each (P31; 6 days of treatment, daily); SEM.

(D–F) AMPA prevents decline in force (D), AMPA delays and CNQX accelerates denervation by FR and S MNs (E), and death (F) in FALS mice. N = 3–5 mice each; SEM.

Daily AMPA treatments from P25 to P31 enhanced MN GADD45β signals, and this effect was much more pronounced in FALS than in wild-type MNs (Figure 3C). Conversely, CNQX reduced MN GADD45β, and the effect of CNQX was more pronounced in wild-type MNs (Figure 3C). AMPA thus enhances the levels of endogenous neuroprotection protein GADD45β in MNs and this upregulation is specifically potentiated in FALS MNs. In contrast to GADD45β, DREAM levels were substantially reduced in FALS MNs compared to wild-type values (Figure 3C). AMPA restored FALS MN DREAM signals to nearly wild-type values, whereas it did not affect DREAM signals in wild-type MNs (Figure 3C). Likewise, CNQX substantially reduced DREAM signals in FALS, but did not affect DREAM signals in wild-type MNs (Figure 3C). Endogenous neuroprotection mechanisms involving DREAM are thus specifically downregulated in FALS MNs, where they are rescued by AMPA and further reduced by CNQX. Finally, Btg2 levels were markedly elevated in FALS MNs, suggesting activation of endogenous neuroprotection pathways (Figure 3C). AMPA restored FALS MN Btg2 to nearly wild-type values, whereas CNQX had no detectable effect (Figure 3C). Taken together, these results provided evidence that AMPA enhances neuroprotection specifically in FALS MNs as revealed by potentiated GADD45β enhancement and by restored FALS MN DREAM levels. The results further suggested that activation of additional neuroprotection pathways in FALS MNs led to elevated Btg2 levels, which were restored to nearly wild-type values by AMPA.

We next determined whether altering AMPA receptor activation also affects clinically relevant disease progression in mutant SOD1 FALS mice. Mutant mice were treated with CNQX or with AMPA from P40 (*G93A-s*) or P20 on (*G93A-f*), and we compared sustained force (grid test), peripheral denervation, and survival in drug-treated and vehicle-treated cohorts. The treatments did not detectably affect total hSOD1 or total pan-SOD1 (mouse plus human) signals in MNs (not shown, but see below). CNQX accelerated force loss (not shown), denervation (Figure 3E) and death (Figure 3F) by ~30 days in mutant SOD1 mice. Prolonged treatments with CNQX did not induce noticeable force loss or denervation in *tgWTSOD1* mice, further supporting the notion that reduced excitability aggravates pathology specifically within a disease background (not shown). Conversely, AMPA markedly improved force (Figure 3D), delayed FR and S denervation (Figure 3E), and extended survival by 20–35 days (Figure 3F) in mutant SOD1 mice. Although denervation by resistant FR and S MNs was substantially delayed by the AMPA receptor treatments, denervation by FF MNs was not detectably affected (not shown, but see below). Likewise, although AMPA receptor activation or inhibition modified the timing of peripheral denervation and clinical manifestations of disease, the same treatments did not alter the specific patterns of progressive deficits involving first the least excitable FF MNs, then FR MNs, and finally the most excitable S MNs. Taken together, these results provided evidence that the status of chronic AMPA receptor activation can modulate disease progression in FALS mice. The results further suggested that FALS FF MNs might be least effective in harnessing neuroprotection through excitability.

Cell Autonomous Neuroprotection by Excitability in FALS MNs

To determine whether excitability specifically of MNs influences misfSOD1 accumulation and disease-related pathology in FALS mice we carried out pharmacogenetic experiments in vivo. Floxed pharmacologically selective actuator module (PSAM) either coupled to 5HT3-receptor (PSAM-Act) for neuronal depolarization or to glycine-receptor (PSAM-Inh) for neuronal hyperpolarization (Magnus et al., 2011) was expressed unilaterally in lumbar spinal cord alpha-MNs (*ChAT-Cre* mice) or Parvalbumin-positive interneurons (PV) (*PV-Cre* mice) using AAV9 viral vectors. Expressed channels were then activated using a specific ligand (Magnus et al., 2011). Unilateral channel expression in individual MNs or PV neurons, including PSAM-expressing PV boutons adjacent to alpha-MNs, could be readily detected with fluorescently labeled α-Bungarotoxin (Figure 4A). Enhancing MN excitability or reducing PV neuron excitability (disinhibition of MNs) specifically reduced misfSOD1 and BiP accumulation in ipsilateral FALS alpha-MNs (Figures 4B and 4C). A detailed analysis revealed that reduced misfSOD1 and BiP accumulation were specifically associated with individual PSAM-expressing MNs within ipsilateral ventral horn (not shown). Total MN hSOD1 signals were not affected in these experiments (Figure 4C). Conversely, reducing MN excitability specifically enhanced misfSOD1 and BiP accumulation in ipsilateral FALS alpha-MNs (Figures 4B and 4C). In control experiments, the same pharmacogenetic treatments did not affect ER stress markers in wild-type MNs (not shown). In parallel to reducing misfSOD1 and BiP accumulation, MN activation specifically enhanced levels of neuroprotective proteins GADD45β and DREAM and decreased Btg2 levels in ipsilateral FALS MNs (Figure 4D). Finally, prolonged pharmacogenetic activation of FALS MNs specifically reduced pEIF2a accumulation (UPR) and delayed muscle denervation by FF MNs (Figure 4E). Taken together, these results provided evidence that enhanced excitability of MNs cell autonomously promotes neuroprotection and delays disease manifestations in FALS MNs.

Altered Signaling to CREB in Affected FALS MNs

To investigate whether intracellular signaling related to excitability might be altered in FALS alpha-MNs, we analyzed MN levels of phosphorylated (Ser133) cAMP response element-binding protein (pCREB), an activity-sensitive readout for alterations in calcium, MAP-kinase, and cAMP pathways in neurons (Greer and Greenberg, 2008). In young presymptomatic FALS mice, pCREB levels within MNs were markedly reduced compared to wild-type mice (Figure 5A). Retrograde labeling revealed that FF MNs exhibited highest pCREB levels among alpha-MNs in resting wild-type mice and that it was specifically FF MNs that exhibited lower pCREB levels in resting FALS mice (Figure 5A). Exercise failed to enhance pCREB levels in FALS MNs (Figure 5A), suggesting diminished excitation-related signaling to CREB in FALS MNs. AMPA reduced pCREB levels in MNs of wild-type and mutant SOD1 mice to comparable levels (Figure 5A). Wild-type and mutant mice treated with the serotonin agonists quizapine (5-HT_{2A}) and 8OH-DPAT (5-$HT_{1A/7}$) also exhibited comparable and substantially reduced pCREB levels in alpha-MNs (Figure 5A), suggesting that enhanced excitability

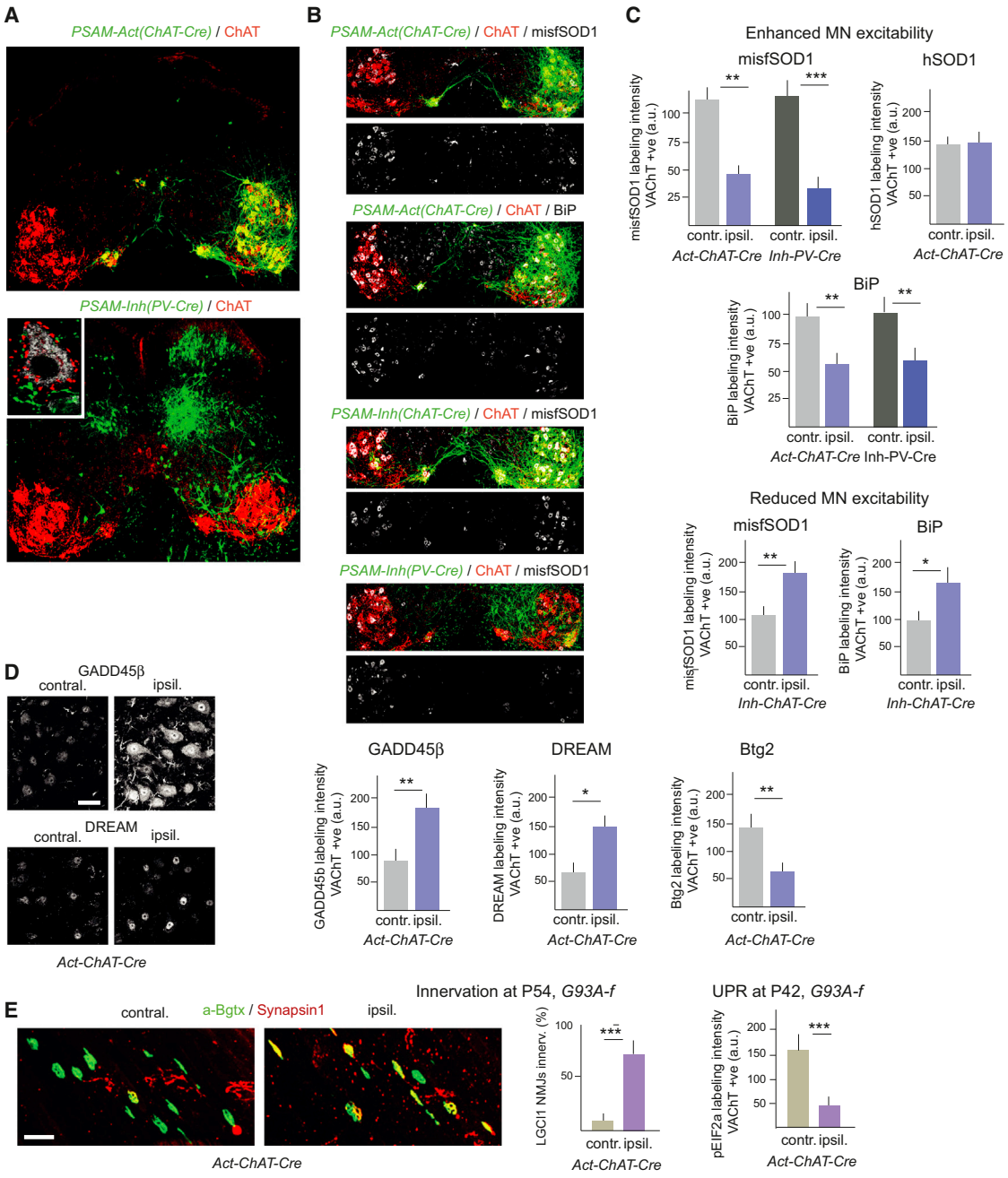

Figure 4. Pharmacogenetic Enhancement of MN Excitability Cell Autonomously Protects FALS MNs

(A) Visualization of PSAM expression in lumbar spinal cord MNs and PV+ interneurons. Note unilateral expression; contralateral expression was restricted to contralaterally extending trunk MNs and PV+ neurons. Inset: PV+ boutons (green) surrounding BiP+ (white)/VAchT-decorated MN.

(B and C) Modulation of misfSOD1 and BiP accumulation in MNs by pharmacogenetically controlled excitability. Total MN hSOD1 signals were not affected (B). Quantitative analysis (C). N = 5 mice each (ipsilateral and contralateral MNs); SEM.

(D) Activation of neuroprotection pathways in FALS MNs upon enhanced MN excitability. N = 4 mice each; SEM. Scale bar represents 20 μm.

(E) Pharmacogenetic enhancement of MN excitability delays UPR in FF MNs and denervation in FF muscle subcompartment. N = 3 (denervation) and N = 4 (UPR) mice each; SEM. Scale bar represents 100 μm.

can neutralize pCREB differences between wild-type and FALS alpha-MN, and reduced pCREB levels in FALS FF MNs at rest might reflect enhanced excitability in these most vulnerable alpha-MNs in early presymptomatic mice.

Enhanced Excitability Connectivity onto FALS MNs

To investigate whether endogenous alterations in excitability connectivity might counteract disease progression in FALS MNs, we analyzed the distribution of synapses that control the

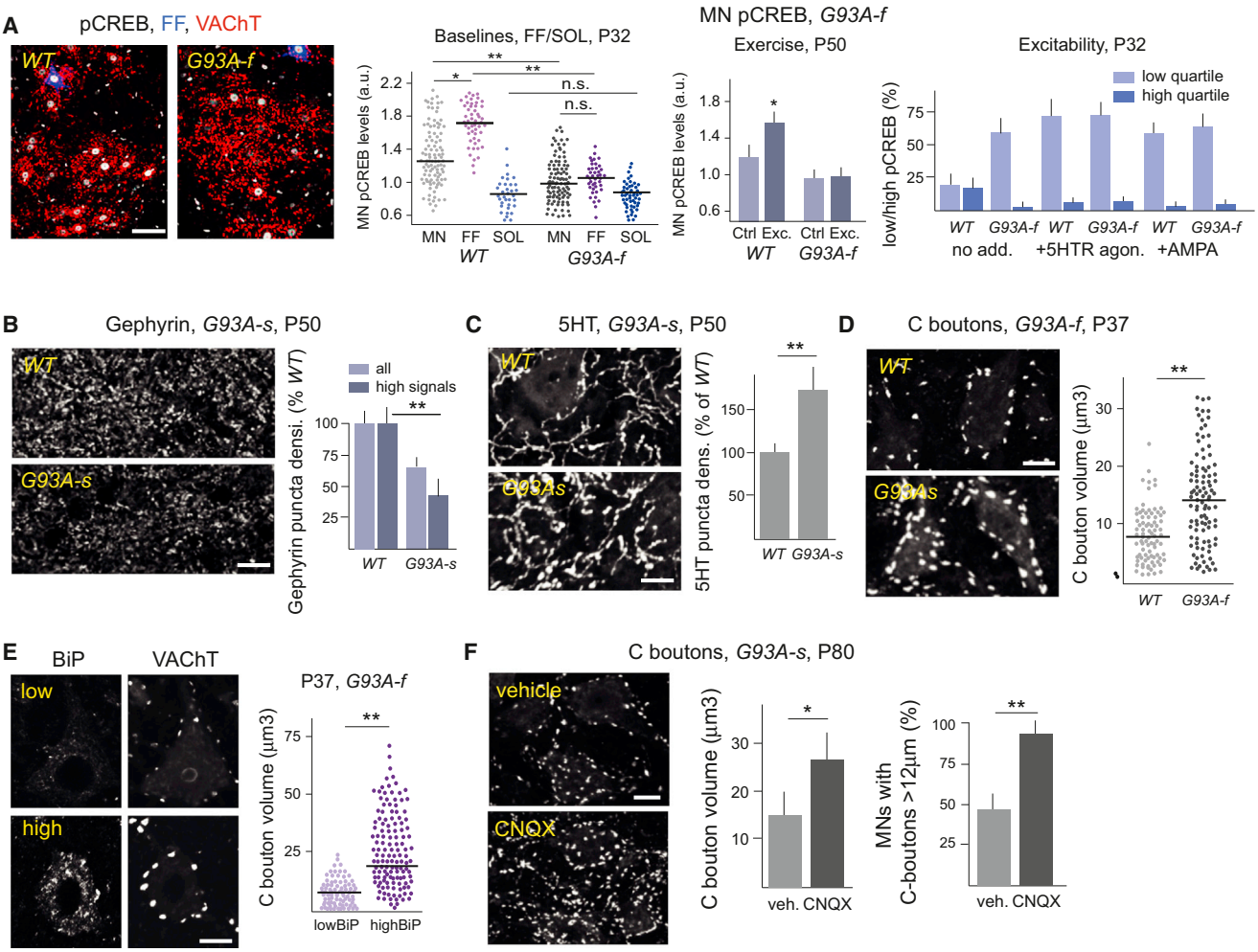

Figure 5. Enhanced Excitability Connectivity onto Vulnerable MNs in FALS Spinal Cord

(A) Reduced pCREB levels in vulnerable FALS FF MNs mimicked by enhanced excitability. Left: retrograde labeling experiment for FF MNs. Note lower pCREB signals in FALS MNs (P32 data). Center left: individual ventral spinal cord MN pCREB signal intensity values (individual dots) from four mice each. Values for vulnerable FF or resistant Soleus MNs identified through retrograde labeling. Center right: average pCREB signal intensity values in wild-type and FALS MNs under resting conditions (Ctrl) and upon treadmill exercise (Exc.); N = 3 mice each; SEM. Right: quantitative analysis; average MN pCREB values for lowest and highest quartiles; N = 3 mice each; SEM. Drug treatments during 2 days. Scale bar represents 50 µm.

(B) Reduced densities of Gephyrin-positive puncta (putative GABAergic synapses) in ventral horn of lumbar spinal cord in FALS mice. N = 3 mice each; SEM. Scale bar represents 25 µm.

(C) Elevated densities of 5HT-positive boutons around alpha-MNs of FALS mice. N = 3 mice each; SEM Scale bar represents 12.5 µm.

(D) Enlarged cholinergic C-boutons surrounding alpha-MNs of FALS mice. N = 3 mice each. Scale bar represents 12.5 µm.

(E) Enlarged C-boutons specifically surrounding vulnerable MNs with enhanced ER stress in presymptomatic FALS mice. Quantitative analysis (individual bouton sizes) from three mice. Scale bar represents 12.5 µm.

(F) AMPA receptor inhibition with CNQX produces further enlargement of C-boutons in FALS mice. CNQX treatment during 5 days; N = 3 mice each; SEM. Scale bar represents 12.5 µm.

excitability of alpha-MNs in FALS mice. We did not detect obvious alterations in the sizes or densities of sensory afferent VGlut1 puncta onto MN somas and proximal dendrites (not shown). By contrast, we found that ventral horn gephyrin puncta densities were 60%–65% of wild-type values (Figure 5B), suggesting a major reduction of inhibitory synapse densities onto mutant MNs at early stages of disease. Furthermore, ventral spinal cord densities of serotonergic boutons, which positively modulate MN excitability and motor output, were significantly elevated in presymptomatic SOD1 mutant mice (Figure 5C). Finally, metabotropic cholinergic C-bouton puncta onto mutant MNs, which also positively modulate MN excitability, were on average substantially larger than in wild-type mice (Figure 5D; see also Pullen and Athanasiou, 2009). These observations suggested the presence of a larger excitability drive onto MNs in early presymptomatic mutant spinal cords.

A more detailed examination of C-bouton size distributions onto individual MNs suggested that only a fraction of the MNs

were contacted by enlarged C-boutons in the mutant mice. Retrograde labeling experiments revealed that in wild-type mice C-boutons contacting FF MNs were larger than those contacting FR or S MNs (not shown) and that it was specifically the C-boutons onto MNs with high BiP signals that were further enlarged in young mutant FALS mice (Figure 5E). An analysis of C-bouton sizes versus age revealed that disease-related enlargement was confined to FF MNs up to their denervation time in *G93A-f* and *G93A-s* mice, when it then extended to a majority of alpha-MNs (not shown). Consistent with a recent report (Herron and Miles, 2012), and with a somewhat more severe progression of disease in male FALS mice, C-bouton enlargements appeared with an 8–10 day delay and were less pronounced in female FALS mice (not shown). CNQX treatment produced C-bouton enlargements in a majority of alpha-MNs in young presymptomatic FALS mice (Figure 5F), supporting the notion that delayed C-bouton enlargement and pathology in FR MNs were related to their higher intrinsic excitability compared to FF MNs. Taken together, these results were consistent with the notion that in FALS mice enhanced excitability connectivity might be induced to provide more effective neuroprotective signaling to vulnerable FALS alpha-MNs.

Neuroprotection in FALS Mediated through Cholinergic C-Bouton Signaling

To investigate endogenous neuroprotective mechanisms that counteract disease progression in FALS mice, we focused on the possible role of C-bouton-mediated neurotransmission onto MNs. Metabotropic transmission at these perisomatic synapses leads to inhibition of calcium-dependent potassium channels, possibly counteracting inhibitory effects of enhanced cytosolic calcium on alpha-MN excitability (Miles et al., 2007; Zagoraiou et al., 2009). Furthermore, these large cholinergic boutons are associated with abundant ER membrane systems closely associated with the postsynaptic membrane, and their enlarged sizes onto the most vulnerable MNs suggested a specific role early in disease (Pullen and Athanasiou, 2009). To determine whether the larger size of C-boutons onto vulnerable MNs of mutant SOD1 mice might occur in response to a deficit in excitability signaling, we analyzed C-bouton size distributions in mice treated with CNQX (Figure 6A). Treating wild-type mice with CNQX produced a substantial and apparently general enlargement of C-boutons (Figures 5F and 6A), whereas AMPA induced a general shrinkage of C-boutons in wild-type mice (Figure 6A). By contrast, reducing ER stress with Salubrinal or enhancing ER stress with Tunicamycin did not influence C-bouton sizes in wild-type or FALS mice (Figure 6A) suggesting that C-bouton sizes adjusted specifically to excitability signaling deficits and not to disease-related ER stress.

To investigate the role of neurotransmission through C-boutons in disease progression, we treated mice with either an antagonist (Methoctramine) or agonist (Oxotremorine) of the type-2 metabotropic ACh receptor, which specifically mediates cholinergic transmission at C-boutons (Miles et al., 2007). Administration of Methoctramine in early presymptomatic FALS mice produced a dramatic increase and spread of misfSOD1 accumulation to most spinal alpha-MNs (Figure 6B). Surprisingly, methoctramine at the same time strongly reduced ER stress and delayed UPR (Figure 6B). Methoctramine initially delayed force loss in presymptomatic mutant mice (Figure 6C), but it later accelerated denervation (Figure 6C), loss of force (Figure 6C) and death (not shown). Conversely, Oxotremorine enhanced BiP signals in MNs (Figure 6D), enhanced UPR in FF MNs (not shown), but did not significantly influence the accumulation of misfSOD1 in FALS MNs (Figure 6D). Oxotremorine delayed denervation (Figure 6E) late loss of force and death (see below) in mutant SOD mice. Although indirect effects of these pharmacological experiments targeting M2 receptors cannot be excluded, the results were consistent with the notion that C-bouton transmission influences disease-related pathology, both in low-excitability FF MNs with enlarged C-boutons, as well as in more resistant FR and S MNs without enlarged C-boutons. In addition, the results revealed a dramatic and unexpected dissociation between the accumulation of misfSOD1 and ER stress in FALS MNs, suggesting that metabotropic cholinergic transmission might influence additional pathways in FALS MNs, accounting for reduced misfSOD1 accumulation and neuroprotection.

Central Neuroprotective Role of mTOR in FALS MNs

In a search for additional neuroprotective pathways that might be activated by metabotropic cholinergic transmission, we noticed that phospho-S6 (pS6) immunoreactivity was specifically elevated in those MNs that exhibited elevated levels of misfSOD1 and BiP (Figure 7A). The elevated pS6 levels reflected enhanced activation of mTOR in those vulnerable MNs, as demonstrated by suppression upon administration of the mTOR inhibitor Rapamycin (Figure 7B), by the concomitant accumulation of the specific mTOR pathway markers p4EBP and pTOR (not shown) and by increased levels of the autophagy markers ATG6/Beclin (Figure 7B) and LC3 (not shown) in FALS MNs upon Rapamycin treatment. FALS MN Btg2 upregulation was abolished in Rapamycin-treated mice (Figure 7B), indicating that it depended on mTOR activation. Elevated pS6 and Btg2 signals were detected in FF MNs from the earliest time points included in our analysis (P15), and increased gradually, in close correspondence with misfSOD1 and BiP, and with larger C-boutons, first exclusively in FF and later also in FR and S MNs (Figure 7C). Methoctramine suppressed and oxotremorine enhanced pS6 (and Btg2, not shown) accumulation in vulnerable MNs (Figure 7D), suggesting that mTOR activation in FALS MNs specifically depended on C-bouton transmission. MN pS6 levels were substantially enhanced by CNQX, suggesting that the C-bouton-mTOR-Btg2 pathway might be activated in FALS MNs in response to a deficit in neuroprotection signaling (Figure 7E).

To determine whether mTOR protects vulnerable MNs against pathology induced by mutant SOD1, we chronically treated FALS mice with Rapamycin and analyzed disease markers in vulnerable MNs. Rapamycin produced a dramatic accumulation of misfSOD1, as well as UPR in most spinal alpha-MNs of presymptomatic mutSOD1 mice (Figure 8A) and a pronounced downregulation of Calreticulin in spinal MNs of presymptomatic FALS mice (Figure 8B), suggesting that the mTOR pathway is critically important to counteract disease-specific pathology in FALS NMs. By contrast, and consistent with the notion that a disease setting involving mutSOD1 specifically renders

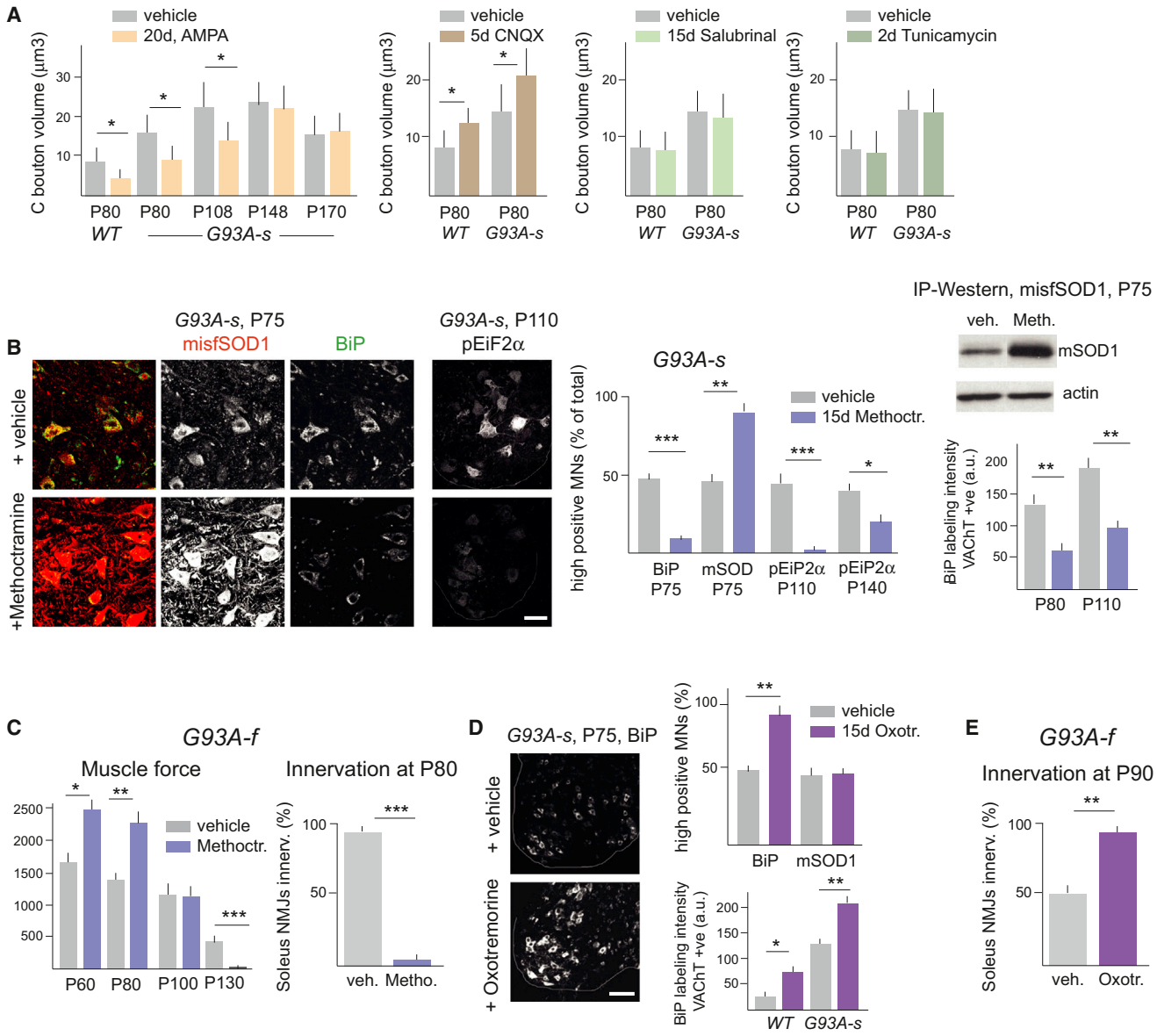

Figure 6. Modulation of Metabotropic Cholinergic Signaling in FALS Mice Reveals Dissociation of misfSOD1 Accumulation and ER Stress in Vulnerable MNs

(A) C-bouton size is inversely correlated to excitability and is not affected by ER stress. N = 100 C-boutons from three mice each; SEM.

(B) Inhibiting metabotropic cholinergic signaling with Methoctramine enhances misfSOD1 accumulation but greatly reduces ER stress in FALS MNs. IP-western: G93A-s mice at P75, previously treated with vehicle or Methoctramine during 15 days. N = 4 mice each; SEM. Scale bar represents 50 µm.

(C) Methoctramine alleviates force loss in early presymptomatic FALS mice, but accelerates denervation by resistant MNs and accelerates force loss in end-stage mice. N = 3 mice (Soleus innervation) and N = 5 mice (force); SEM.

(D) Enhancing metabotropic cholinergic signaling with Oxotremorine augments ER stress, but does not significantly affect misfSOD1 accumulation in FALS MNs. N = 3 mice each; SEM. Scale bar represents 100 µm.

(E) Oxotremorine delays Soleus denervation in FALS mice. N = 4 mice each; SEM.

alpha-MNs dependent on neuroprotection involving mTOR, Rapamycin did not induce ER stress in alpha-MNs of wild-type mice (Figure S1).

To determine whether endogenous mTOR activation protects against clinical aspects of disease progression in mutant SOD1 mice, we compared cohorts of mice treated with Rapamycin or vehicle. Rapamycin produced a complete denervation of soleus muscle at P75 in *G93A-f* mice (Figure 8C), indicating that denervation of FR and S MNs in the mutant mice was accelerated by ~20 and ~60 days, respectively. Furthermore, treating mutant SOD1 mice with Rapamycin decreased survival by ~30 days (not shown; N = 5 mice each, $p < 0.001$). By contrast, and

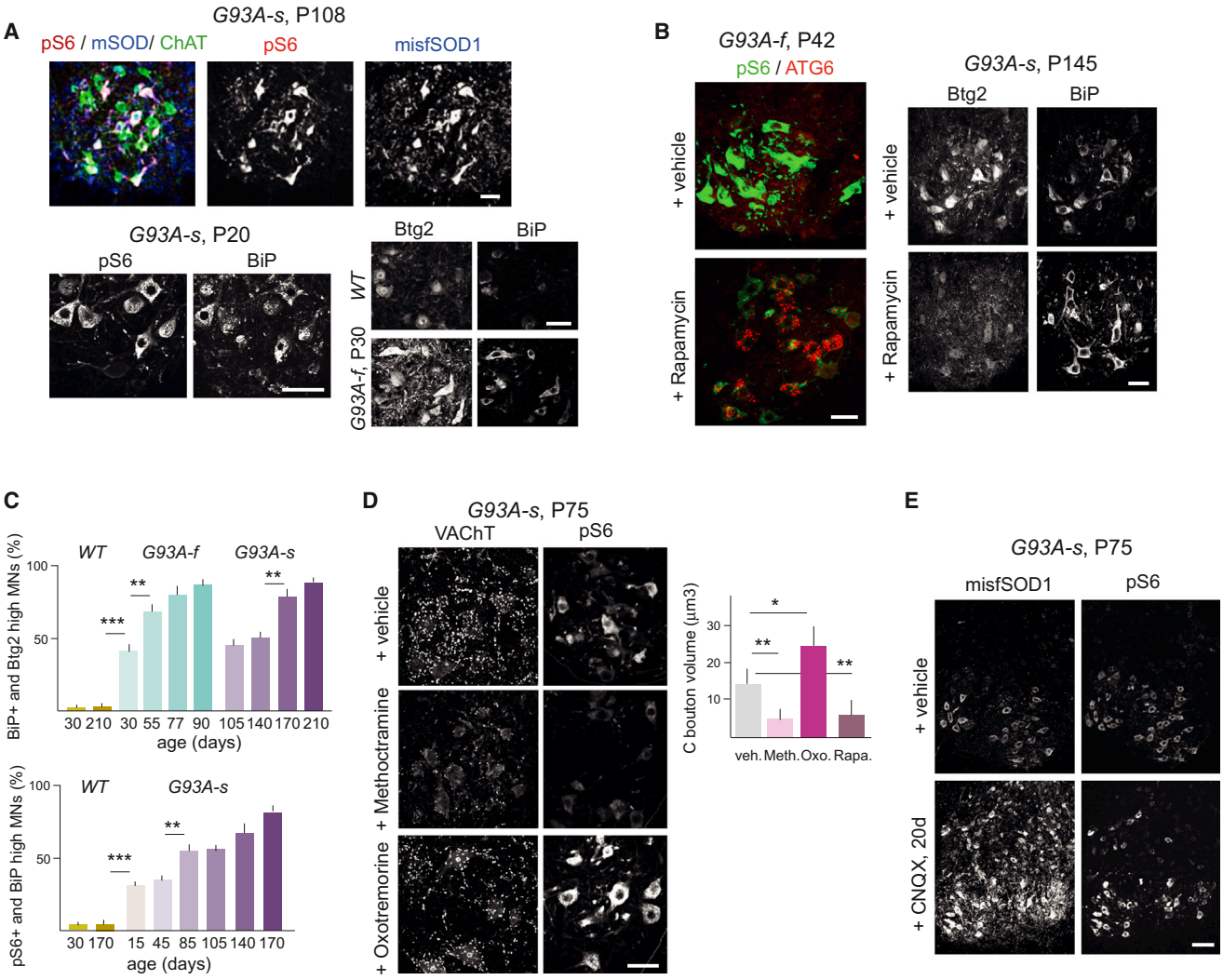

Figure 7. Early mTOR Activation Specifically in Vulnerable FALS MNs and Dependence on Metabotropic Cholinergic Signaling

(A) Accumulation of pS6 and Btg2 immunoreactivity specifically in vulnerable (high BiP, high misfSOD1) FALS MNs. Scale bar represents 50 μm.

(B) mTOR activation in vulnerable FALS MNs and mTOR-dependent expression of calcium-regulated neuroprotective transcriptional coactivator Btg2. Rapamycin treatment: 15 days. Scale bar represents 50 μm.

(C) Disease-related accumulation of pS6 and Btg2 in vulnerable FALS MNs. N = 3–5 mice each; SEM.

(D) Metabotropic cholinergic signaling loops: mTOR activation in FALS MNs depends on metabotropic cholinergic signaling, and C-bouton volume is positively modulated by M2 and mTOR signaling. N = 3 mice and 100 C-boutons each; SEM. Scale bar represents 50 μm.

(E) Chronic inhibition of AMPA receptor activation induces ER stress in most FALS neurons, but enhanced mTOR activation only in FALS MNs. Scale bar represents 100 μm.

consistent with the notion that vulnerable MNs depend on active mTOR for neuroprotection specifically within a FALS setting, chronic treatment of wild-type mice with Rapamycin did not detectably affect peripheral innervation (Figure S1) or survival (not shown). Taken together, these results suggested that metabotropic cholinergic transmission promotes distinct processes in MNs, with opposite impacts on MN pathology in a FALS context; these include neuroprotective mTOR activation and pathology-enhancing ER stress activation.

To determine whether mTOR activation downstream of metabotropic cholinergic transmission is important to protect MNs in disease, we analyzed mutant SOD1 mice treated chronically with Oxotremorine to stimulate mTOR and at the same time with Salubrinal to reduce the concomitant elevation of ER stress. The dual treatment dramatically delayed pathology and clinical manifestations in FALS mice. Thus, Oxotremorine + Salubrinal greatly reduced the accumulation of misfSOD1 (Figure 8D), reduced ER stress markers (Figure 8D), and delayed UPR (not shown), while preserving elevated levels of pS6 and Btg2 (not shown) in FALS MNs. In parallel, Oxotremorine + Salubrinal delayed peripheral denervation of FR and S MNs by at least 40 days, substantially counteracted force loss, and extended survival by 50 ± 9 days (N = 8 mice each, $p < 0.0001$) in the FALS mice (Figure 8E).

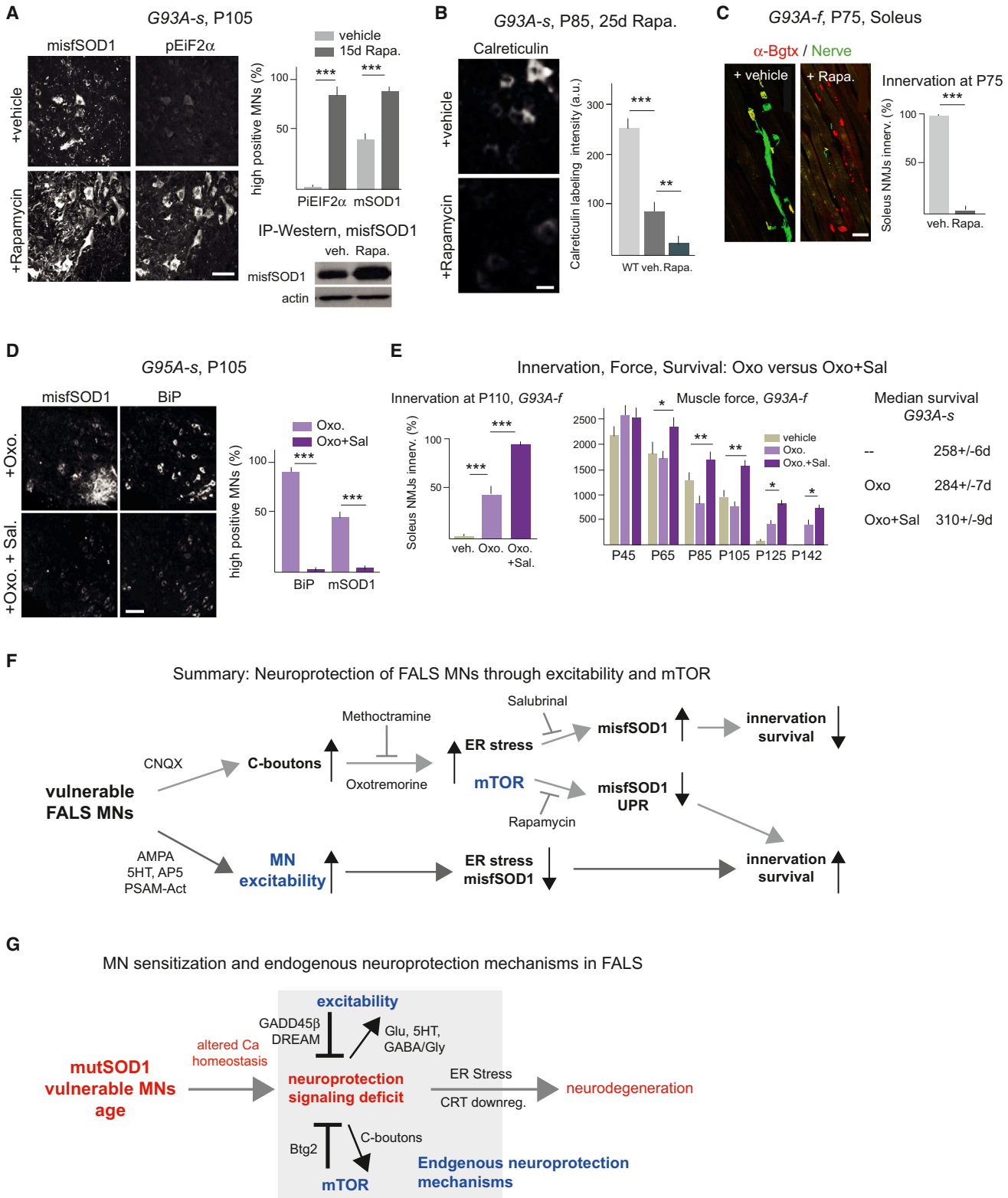

Figure 8. mTOR Signaling Provides Endogenous Neuroprotection and Delays Disease Progression in FALS Mice

(A) Enhanced misfSOD1 accumulation and UPR in a majority of spinal MNs upon treatment of FALS mice with Rapamycin. Rapamycin: every second day, for 15 days. N = 3 mice each; SEM. Scale bar represents 50 μm.

(legend continued on next page)

DISCUSSION

We have investigated early mechanisms of disease in SOD1 mouse models of FALS, focusing on endogenous neuroprotection mechanisms and the selective vulnerability of alpha-MNs. We provide evidence that disease-associated SOD1 mutants specifically render vulnerable MNs dependent on endogenous neuroprotection signaling involving MN excitability and mTOR. The most vulnerable low-excitability FF MNs exhibited evidence of pathology and neuroprotection recruitment from P7–14 on, which included increasing accumulation of misfSOD1 and enhanced mTOR activation. Enhancing MN excitability was sufficient to reverse misfSOD1 accumulation, whereas blocking metabotropic cholinergic signaling greatly enhanced misfSOD1 accumulation in alpha-MNs but reduced ER stress, suggesting that ER stress is not directly caused by misfSOD1 accumulation in FALS (Figure 8F). During a protracted presymptomatic phase, inhibiting excitability was sufficient to induce comparable pathology and enhanced neurocompensatory responses in most alpha-MNs, but not in other neurons in FALS mice, suggesting that the relatively higher resilience of FR and S alpha-MNs to disease is related to their comparatively higher excitabilities. Modulating excitability and/or alpha-MN mTOR influenced the progression rates of motor dysfunction, muscle denervation, and death, providing evidence that excitability and mTOR are key endogenous mechanisms to counteract clinically important disease progression in FALS (Figures 8F and 8G). In the following sections, we discuss the main implications of these results and how they relate to those of previous studies addressing mechanisms of disease in neurodegeneration.

Selective Vulnerability of MNs to SOD-Mediated Neurodegeneration

Our results provide insights as to how MNs are selectively affected in FALS. Because most neurons accumulated misfSOD1 in FALS mice treated chronically with CNQX, but not in *tgwtSOD1* mice, our results do not support the notion that this ubiquitously expressed mutant protein specifically affects alpha-MNs. Instead, our results suggest that SOD1 mutants alter aspects of homeostasis signaling related to excitability that are particularly consequential in vulnerable alpha-MNs (Figure 8G). Thus, short-term global inhibition of excitability during 1–3 days in mutant SOD1 FALS mice induced misfSOD1 accumulation and a robust UPR in most alpha-MNs, but not in other neurons in the spinal cord or in the brain. Furthermore, direct pharmacogenetic inhibition of excitability in MNs enhanced misfSOD1 accumulation and ER stress in those MNs. Taken together, our findings suggest that in mutSOD1 models of FALS vulnerable alpha-MNs are highly sensitized to cellular stressors and specifically depend on endogenous excitability and mTOR to delay clinically relevant disease progression (Figure 8G). This sensitization model of motoneuron disease pathophysiology suggests that the signaling and homeostasis networks of vulnerable alpha-MNs include specific features that render these neurons more susceptible to neurodegeneration pathways (Kanning et al., 2010; Saxena and Caroni, 2011). These might be closely linked to calcium homeostasis processes (von Lewinski and Keller, 2005; Kanning et al., 2010; Bernard-Marissal et al., 2012). The model is reminiscent of findings in Parkinson's, Alzheimer's, and Huntington's disease studies, in which specific neuronal vulnerabilities have also been related to selective degeneration (Bezprozvanny and Mattson, 2008; Mosharov et al., 2009; Saxena and Caroni, 2011; Gleichmann et al., 2012). As discussed below, alterations in calcium fluxes and excitability signaling might be a common pathogenic signature of neurodegenerative diseases.

Although our results suggest that the particular vulnerability of alpha-MNs to neurodegeneration involves excitability-related pathways, the specific homeostasis and signaling pathway features that account for this higher vulnerability remain to be determined. The conclusions of our study in FALS mice are consistent with those of previous studies reporting that vulnerable FALS MNs in vitro are specifically susceptible to cell death induced by Fas-ligand and nitric oxide, whereas wild-type MNs or other FALS neurons are not (Raoul et al., 2002). Like the present study, those studies concluded that FALS MNs acquire a vulnerability to specific stressors not present in wild-type MNs. Those studies further provided evidence that elevated cytosolic calcium levels and loss of Calreticulin are critical determinants of enhanced vulnerability in cultured FALS MNs, leading to ER stress and cell death (Bernard-Marissal et al., 2012). We detected similar Calreticulin downregulation correlated with advancing pathology and inhibited by excitability and mTOR in our study, consistent with the notion that imbalances in alpha-MN calcium homeostasis might underlie disease progression in FALS mice (Figure 8G).

Endogenous Neuroprotection Analysis Reveals Mechanisms of Disease Progression

Our longitudinal study in FALS mice provides experimental evidence as to endogenous neuroprotection mechanisms that delay pathology and dysfunction in FALS and suggests that a deficit in excitability signaling in vulnerable alpha-MNs might

(B) Rapamycin induces further reduction of Calreticulin expression in FALS MNs. N = 3 mice each; SEM. Scale bar represents 25 μm.
(C) Accelerated denervation by resistant Soleus MNs upon Rapamycin treatment (20 days). N = 3 mice each; SEM. Scale bar represents 100 μm.
(D) Combination treatment with Oxotremorine and Salubrinal greatly reduces misfSOD1 accumulation and ER stress in presymptomatic FALS mice. Treatment duration: 15 days. N = 4 mice each; SEM. Scale bar represents 100 μm.
(E) Delayed Soleus denervation, force loss and death in FALS mice treated with Oxotremorine and Salubrinal. All treatments were from P30 on. N = 8 mice each; SEM.
(F) Summary of how MN excitability and metabotropic cholinergic signaling influence pathology in FALS MNs. Endogenous neuroprotection processes in blue.
(G) Proposed model of vulnerable MN sensitization to stressors and role of endogenous neuroprotection mechanisms in FALS. Endogenous neuroprotection processes in blue, against gray background. CRT: Calreticulin; Glu, 5HT, GABA/Gly, C-boutons: synaptic pathways promoting endogenous neuroprotection. Metabotropic cholinergic activation also enhances ER stress, and enhanced excitability might also augment neurotoxicity.
See also Figure S2.

be a key disease-driving factor in ALS. Contrary to some previous reports, our findings suggest that the well-documented early hyperexcitability of MNs in ALS (Vucic et al., 2008; Piotrkiewicz and Hausmanowa-Petrusewicz, 2011; Martin and Chang, 2012) might represent an adaptive response to boost neuroprotective signaling in alpha-MNs (see also Gordon et al., 2010). Indeed, initial hypoexcitability of FALS MNs has been reported by some studies (Bories et al., 2007). At the same time, however, hyperexcitability might contribute to aggravate disease loads on MNs through excitotoxicity mechanisms (Rothstein, 1995-1996; Van Den Bosch et al., 2006; Gleichmann et al., 2012). Our results further provide a conceptual framework to account for the particularly high vulnerability of low-excitability FF MNs to disease (Pun et al., 2006; Saxena et al., 2009). The results suggest that in addition to being affected earliest in disease, high-threshold FF MNs might be less effective in coupling excitability to neuroprotection, leading to less effective delay of denervation with AMPA or Oxotremorine + Salubrinal in FF MNs. Comparable vulnerability sequences involving first FF and last S MNs have also been reported for the juvenile motoneuron disease SMA and for motoneuron dysfunctions associated with aging (Kanning et al., 2010; Valdez et al., 2012), suggesting that signaling related to excitability might be a central target of dysfunction in neurodegenerative conditions affecting MNs (Mentis et al., 2011; Imlach et al., 2012).

Contrary to some (Ravikumar et al., 2004), but not all (Zhang et al., 2011; Kim et al., 2012; Selvaraj et al., 2012) previous studies on the role of mTOR signaling in neurodegeneration, our results provide evidence that mTOR activity is critically important to delay disease progression in FALS. mTOR-dependent accumulation of the potent neuroprotective gene Btg2, a calcium-induced transcriptional coregulator, suggests that mTOR signaling might be required to boost compromised neuroprotective signaling pathways in FALS MNs, thereby synergizing with excitability signaling (Greer and Greenberg, 2008; Zhang et al., 2009; Hardingham and Bading, 2010) (Figures 8F and 8G). Enhancing MN excitability was sufficient to reverse Btg2 upregulation, suggesting that a protective mTOR-Btg2 pathway is augmented in FALS MNs upon a deficit in neuroprotective signaling through excitability. Given that Rapamycin appears to be protective in some neurodegenerative settings (e.g., by relieving a brake on autophagy), the mTOR pathway might provide neuroprotection specifically within certain disease contexts including FALS, but might interfere with neuroprotection in a different subset of disease contexts. Our findings further suggest that although misfSOD1 accumulation is a valuable biomarker of disease (Bosco et al., 2010) (Figure 8G), it might not directly promote disease progression. Indeed, one interpretation consistent with our results is that misfSOD1 accumulation in MNs might be part of a cellular defense process to trap and neutralize dysfunctional components in larger aggregates (Arrasate et al., 2004). The accumulation of misfSOD1 was most closely correlated to a deficit in excitability signaling in vulnerable FALS MNs (Piotrkiewicz and Hausmanowa-Petrusewicz, 2011), suggesting that mutSOD1 might interact and interfere with molecular components involved in neuronal excitability, e.g., proteins affecting calcium transport (Kikuchi et al., 2006; Urushitani et al., 2008; Rizzuto et al., 2012).

Our observations that enhanced excitability and mTOR are critically important to provide neuroprotection in FALS MNs are consistent with the notion that altered calcium fluxes, e.g., through the ER might underlie the enhanced vulnerability of alpha-MNs in FALS mice (Siklós et al., 1998; Langou et al., 2010). Reduced ER calcium and elevated cytosolic calcium might reduce the excitability of FALS MNs due to hyperpolarization of the plasma membrane through calcium-dependent potassium currents, and inhibition of these currents might provide one mechanism through which C-boutons protect alpha-MNs in FALS. The larger C-boutons might augment calcium refilling in FALS alpha-MNs (Pullen and Athanasiou, 2009), e.g., through store-operated calcium entry involving ER membranes at C-boutons (Shen et al., 2011), but voltage-gated calcium channel routes are also possible. Similar mechanisms relating calcium fluxes and excitability to neurodegeneration and neuroprotection might be relevant to other neurodegenerative diseases (Tu et al., 2006; Palop and Mucke, 2010; Gleichmann et al., 2012). Thus, reduced ER calcium levels and calcium gradients across the ER as well as Calreticulin downregulation have also been related to disease in Alzheimer's, Parkinson's, and Huntington's disease (Taguchi et al., 2000; Kipanyula et al., 2012). Furthermore, excitability and synaptic calcium entry have been related to neuroprotective signaling (Hardingham and Bading, 2010).

In conclusion, our results provide insights into causal relationships between critical early disease-related dysfunctions and adaptive responses in FALS mice. We identify excitability signaling and a synaptic and molecular pathway leading to mTOR activation in alpha-MNs as critically important to provide neuroprotection in FALS MNs. More generally, our results provide evidence that a focus on endogenous neuroprotection pathways in presymptomatic mice can provide valuable and unbiased criteria to assess the potential of therapeutic strategies in neurodegeneration.

EXPERIMENTAL PROCEDURES

Mice, Reagents, and Pharmacological Treatments

B6SJL-TgN(SOD1-G93A)^{dl}1Gur/J, referred to as slow (*G93A-s*), B6SJL-Tg(SOD1-G93A)1Gur/J, referred to as fast (*G93A-f*), and B6SJL-Tg(SOD1-G85R) were obtained from Jackson Laboratory. *ChAT-CRE* and *PV-CRE* mice were from S. Arber (Biozentrum and FMI). All experiments were carried out in male mice. Animal housing, care, and experimental procedures were conformed to Swiss Veterinary Law guidelines.

Drug delivery regimes were based on published reports. In addition, dose-response curves were established in FALS mice in order to avoid detectable toxicity ranges in the mutant mice (at least one order of magnitude below toxic dosages; see Supplemental Experimental Procedures). Drug delivery protocols in all mice were as follows. Methoctramine (Sigma): injected intraperitoneally (i.p.) in saline at 200 μg/kg; Salubrinal (Alexis Biochemicals; dissolved at 10 mg/ml in DMSO) injected i.p. in saline at 1 mg/kg; Oxotremorine M (Tocris Bioscience) injected i.p. in saline at 30–50 μg/kg; Rapamycin (Tocris Bioscience; dissolved in ethanol at 20 mg/ml) injected i.p. in adjuvant at 6 mg/kg; (RS)-AMPA hydrobromide (Tocris Bioscience) injected i.p. in saline (or in sweetened drinking water, at 6 nM/l) at 15–20 nM/25 gm (or 3 nM/l in sweetened drinking water for chronic treatments); CNQX at 20 μmol/l drinking water; Tunicamycin, Brefeldin, Thapsigargin (Ascent Scientific) injected i.p. in saline at 1 μg/g; Quizapine (Tocris) injected i.p. in saline at 0.3 mg/kg; 8OHDPAT (Tocris) injected subcutaneously (s.c.) in saline at 0.3 mg/kg; Ketanserin (Tocris) injected s.c. in saline at 5 mg/kg; and WAY100135 (Tocris) injected s.c. in saline at 5 mg/kg.

For pharmacogenetic experiments, pAAV(9)-CBA-GFP-2A-floxed-PSAM(L141F,Y115F)GlyR-WPRE at the titer of 6.3 × 10^{13} and pAAV(9)-pCAG-A7-floxed-PSAM(L141F, Y115F)5HT3-WPRE at the titer of 9 × 10^{13} were prepared by Vector BioLabs as described (Magnus et al., 2011). A total of 1 μl of viral suspension was injected during 30 min with a glass capillary coupled to a Picospritzer-III apparatus in 8–10 ms pulses (Supplemental Experimental Procedures). The ligand JFRC-PSEM-0308 (kind gift of S. Sternson) was administered by daily i.p. injections at the dose of 5 mg/kg in saline, starting 5 days after viral injection.

Immunocytochemistry and Antibodies

Mice were perfused with 4% PFA in PBS, (L3–L5) lumbar spinal cord or cerebellum was isolated and kept overnight at 4°C in 30% sucrose. After embedding, 50 μm cryostat sections were post fixed with 4% PFA for 10 min, followed by PBS washes. Antibodies (Supplemental Experimental Procedures) were applied in PBS with 3% BSA, 0.3% Triton X-100, and incubated either overnight or for 3 days at 4°C. Sections were then briefly washed with PBS and incubated for 120 min at room temperature with appropriate combinations of secondary antibodies from Invitrogen.

Imaging and Image Analyses

Confocal images were acquired using a Leica SP5 (Leica Microsystems), fitted with a 20× air objective, Olympus Fluoview (Olympus, Tokyo) microscope, fitted with a 10× or 20× air objective, or an LSM Meta (Carl Zeiss AG) microscope, fitted with a 40× oil objective. Images were processed using Imaris software (Supplemental Experimental Procedures).

For the analysis of BiP or misf-SOD1 labeling intensities, data were acquired using identical confocal settings, ensuring that signals at the brightest cells were not saturated and that background levels outside MN pools were still detectable. Images were analyzed quantitatively using Image-Pro 5 software (Media Cybernetics). Signal intensities were measured at several regions within areas inside cells (at least three regions per cell), excluding areas lacking signal; average intensities were calculated and background levels outside cells were subtracted from these values. For the calculation of MN percentages expressing misf-SOD1, BiP, P_i-eIF2α, or p-S6, double positive MNs (MN markers were ChAT or VAChT) and signal intensity values for the antigen of interest were calculated over 15–20 spinal sections in triplicate animals (Supplemental Experimental Procedures).

SUPPLEMENTAL INFORMATION

Supplemental Information includes Supplemental Experimental Procedures and two figures and can be found with this article online at http://dx.doi.org/10.1016/j.neuron.2013.07.027.

ACKNOWLEDGMENTS

We are grateful to K. McAllister and C. Gee (Novartis Institutes for Biomedical Research, Basel) for suggestions and help with the original AMPA receptor antagonist experiments and to S. Sternson (Janelia Farms) for the pharmacogenetic reagents. The Friedrich Miescher Institute for Biomedical Research is supported by the Novartis Research Foundation. F.R. was supported by an EMBO long-term fellowship; F. G.-L. and J.-P. J. were supported by the Canadian Institutes of Health Research.

Accepted: July 17, 2013
Published: September 18, 2013

REFERENCES

Arrasate, M., Mitra, S., Schweitzer, E.S., Segal, M.R., and Finkbeiner, S. (2004). Inclusion body formation reduces levels of mutant huntingtin and the risk of neuronal death. Nature *431*, 805–810.

Bernard-Marissal, N., Moumen, A., Sunyach, C., Pellegrino, C., Dudley, K., Henderson, C.E., Raoul, C., and Pettmann, B. (2012). Reduced calreticulin levels link endoplasmic reticulum stress and Fas-triggered cell death in motoneurons vulnerable to ALS. J. Neurosci. *32*, 4901–4912.

Bezprozvanny, I., and Mattson, M.P. (2008). Neuronal calcium mishandling and the pathogenesis of Alzheimer's disease. Trends Neurosci. *31*, 454–463.

Boillée, S., Vande Velde, C., and Cleveland, D.W. (2006). ALS: a disease of motor neurons and their nonneuronal neighbors. Neuron *52*, 39–59.

Bories, C., Amendola, J., Lamotte d'Incamps, B., and Durand, J. (2007). Early electrophysiological abnormalities in lumbar motoneurons in a transgenic mouse model of amyotrophic lateral sclerosis. Eur. J. Neurosci. *25*, 451–459.

Bosco, D.A., Morfini, G., Karabacak, N.M., Song, Y., Gros-Louis, F., Pasinelli, P., Goolsby, H., Fontaine, B.A., Lemay, N., McKenna-Yasek, D., et al. (2010). Wild-type and mutant SOD1 share an aberrant conformation and a common pathogenic pathway in ALS. Nat. Neurosci. *13*, 1396–1403.

Ezzi, S.A., Urushitani, M., and Julien, J.P. (2007). Wild-type superoxide dismutase acquires binding and toxic properties of ALS-linked mutant forms through oxidation. J. Neurochem. *102*, 170–178.

Gleichmann, M., Zhang, Y., Wood, W.H., 3rd, Becker, K.G., Mughal, M.R., Pazin, M.J., van Praag, H., Kobilo, T., Zonderman, A.B., Troncoso, J.C., et al. (2012). Molecular changes in brain aging and Alzheimer's disease are mirrored in experimentally silenced cortical neuron networks. Neurobiol. Aging *33*, e1–e18.

Gordon, T., Tyreman, N., Li, S., Putman, C.T., and Hegedus, J. (2010). Functional over-load saves motor units in the SOD1-G93A transgenic mouse model of amyotrophic lateral sclerosis. Neurobiol. Dis. *37*, 412–422.

Greer, P.L., and Greenberg, M.E. (2008). From synapse to nucleus: calcium-dependent gene transcription in the control of synapse development and function. Neuron *59*, 846–860.

Gros-Louis, F., Soucy, G., Larivière, R., and Julien, J.P. (2010). Intracerebroventricular infusion of monoclonal antibody or its derived Fab fragment against misfolded forms of SOD1 mutant delays mortality in a mouse model of ALS. J. Neurochem. *113*, 1188–1199.

Gurney, M.E., Pu, H., Chiu, A.Y., Dal Canto, M.C., Polchow, C.Y., Alexander, D.D., Caliendo, J., Hentati, A., Kwon, Y.W., Deng, H.X., et al. (1994). Motor neuron degeneration in mice that express a human Cu,Zn superoxide dismutase mutation. Science *264*, 1772–1775.

Hardingham, G.E., and Bading, H. (2010). Synaptic versus extrasynaptic NMDA receptor signalling: implications for neurodegenerative disorders. Nat. Rev. Neurosci. *11*, 682–696.

Herron, L.R., and Miles, G.B. (2012). Gender-specific perturbations in modulatory inputs to motoneurons in a mouse model of amyotrophic lateral sclerosis. Neuroscience *226*, 313–323.

Imlach, W.L., Beck, E.S., Choi, B.J., Lotti, F., Pellizzoni, L., and McCabe, B.D. (2012). SMN is required for sensory-motor circuit function in Drosophila. Cell *151*, 427–439.

Kanekura, K., Suzuki, H., Aiso, S., and Matsuoka, M. (2009). ER stress and unfolded protein response in amyotrophic lateral sclerosis. Mol. Neurobiol. *39*, 81–89.

Kanning, K.C., Kaplan, A., and Henderson, C.E. (2010). Motor neuron diversity in development and disease. Annu. Rev. Neurosci. *33*, 409–440.

Kikuchi, H., Almer, G., Yamashita, S., Guégan, C., Nagai, M., Xu, Z., Sosunov, A.A., McKhann, G.M., 2nd, and Przedborski, S. (2006). Spinal cord endoplasmic reticulum stress associated with a microsomal accumulation of mutant superoxide dismutase-1 in an ALS model. Proc. Natl. Acad. Sci. USA *103*, 6025–6030.

Kim, S.R., Kareva, T., Yarygina, O., Kholodilov, N., and Burke, R.E. (2012). AAV transduction of dopamine neurons with constitutively active Rheb protects from neurodegeneration and mediates axon regrowth. Mol. Ther. *20*, 275–286.

Kipanyula, M.J., Contreras, L., Zampese, E., Lazzari, C., Wong, A.K.C., Pizzo, P., Fasolato, C., and Pozzan, T. (2012). Ca^{2+} dysregulation in neurons from transgenic mice expressing mutant presenilin 2. Aging Cell *11*, 885–893.

Kok, E., Haikonen, S., Luoto, T., Huhtala, H., Goebeler, S., Haapasalo, H., and Karhunen, P.J. (2009). Apolipoprotein E-dependent accumulation of Alzheimer disease-related lesions begins in middle age. Ann. Neurol. *65*, 650–657.

Langou, K., Moumen, A., Pellegrino, C., Aebischer, J., Medina, I., Aebischer, P., and Raoul, C. (2010). AAV-mediated expression of wild-type and ALS-linked mutant VAPB selectively triggers death of motoneurons through a Ca2+-dependent ER-associated pathway. J. Neurochem. *114*, 795–809.

Magnus, C.J., Lee, P.H., Atasoy, D., Su, H.H., Looger, L.L., and Sternson, S.M. (2011). Chemical and genetic engineering of selective ion channel-ligand interactions. Science *333*, 1292–1296.

Martin, L.J., and Chang, Q. (2012). Inhibitory synaptic regulation of motoneurons: a new target of disease mechanisms in amyotrophic lateral sclerosis. Mol. Neurobiol. *45*, 30–42.

Mentis, G.Z., Blivis, D., Liu, W., Drobac, E., Crowder, M.E., Kong, L., Alvarez, F.J., Sumner, C.J., and O'Donovan, M.J. (2011). Early functional impairment of sensory-motor connectivity in a mouse model of spinal muscular atrophy. Neuron *69*, 453–467.

Miles, G.B., Hartley, R., Todd, A.J., and Brownstone, R.M. (2007). Spinal cholinergic interneurons regulate the excitability of motoneurons during locomotion. Proc. Natl. Acad. Sci. USA *104*, 2448–2453.

Molinari, M., Eriksson, K.K., Calanca, V., Galli, C., Cresswell, P., Michalak, M., and Helenius, A. (2004). Contrasting functions of calreticulin and calnexin in glycoprotein folding and ER quality control. Mol. Cell *13*, 125–135.

Mosharov, E.V., Larsen, K.E., Kanter, E., Phillips, K.A., Wilson, K., Schmitz, Y., Krantz, D.E., Kobayashi, K., Edwards, R.H., and Sulzer, D. (2009). Interplay between cytosolic dopamine, calcium, and alpha-synuclein causes selective death of substantia nigra neurons. Neuron *62*, 218–229.

Palop, J.J., and Mucke, L. (2010). Amyloid-beta-induced neuronal dysfunction in Alzheimer's disease: from synapses toward neural networks. Nat. Neurosci. *13*, 812–818.

Piotrkiewicz, M., and Hausmanowa-Petrusewicz, I. (2011). Motoneuron afterhyperpolarisation duration in amyotrophic lateral sclerosis. J. Physiol. *589*, 2745–2754.

Pokrishevsky, E., Grad, L.I., Yousefi, M., Wang, J., Mackenzie, I.R., and Cashman, N.R. (2012). Aberrant localization of FUS and TDP43 is associated with misfolding of SOD1 in amyotrophic lateral sclerosis. PLoS ONE *7*, e35050.

Pullen, A.H., and Athanasiou, D. (2009). Increase in presynaptic territory of C-terminals on lumbar motoneurons of G93A SOD1 mice during disease progression. Eur. J. Neurosci. *29*, 551–561.

Pun, S., Santos, A.F., Saxena, S., Xu, L., and Caroni, P. (2006). Selective vulnerability and pruning of phasic motoneuron axons in motoneuron disease alleviated by CNTF. Nat. Neurosci. *9*, 408–419.

Raoul, C., Estévez, A.G., Nishimune, H., Cleveland, D.W., deLapeyrière, O., Henderson, C.E., Haase, G., and Pettmann, B. (2002). Motoneuron death triggered by a specific pathway downstream of Fas. potentiation by ALS-linked SOD1 mutations. Neuron *35*, 1067–1083.

Ravikumar, B., Vacher, C., Berger, Z., Davies, J.E., Luo, S., Oroz, L.G., Scaravilli, F., Easton, D.F., Duden, R., O'Kane, C.J., and Rubinsztein, D.C. (2004). Inhibition of mTOR induces autophagy and reduces toxicity of polyglutamine expansions in fly and mouse models of Huntington disease. Nat. Genet. *36*, 585–595.

Reiman, E.M., Chen, K., Alexander, G.E., Caselli, R.J., Bandy, D., Osborne, D., Saunders, A.M., and Hardy, J. (2004). Functional brain abnormalities in young adults at genetic risk for late-onset Alzheimer's dementia. Proc. Natl. Acad. Sci. USA *101*, 284–289.

Rizzuto, R., De Stefani, D., Raffaello, A., and Mammucari, C. (2012). Mitochondria as sensors and regulators of calcium signalling. Nat. Rev. Mol. Cell Biol. *13*, 566–578.

Rothstein, J.D. (1995-1996). Excitotoxicity and neurodegeneration in amyotrophic lateral sclerosis. Clin. Neurosci. *3*, 348–359.

Saxena, S., and Caroni, P. (2011). Selective neuronal vulnerability in neurodegenerative diseases: from stressor thresholds to degeneration. Neuron *71*, 35–48.

Saxena, S., Cabuy, E., and Caroni, P. (2009). A role for motoneuron subtype-selective ER stress in disease manifestations of FALS mice. Nat. Neurosci. *12*, 627–636.

Selvaraj, S., Sun, Y., Watt, J.A., Wang, S., Lei, S., Birnbaumer, L., and Singh, B.B. (2012). Neurotoxin-induced ER stress in mouse dopaminergic neurons involves downregulation of TRPC1 and inhibition of AKT/mTOR signaling. J. Clin. Invest. *122*, 1354–1367.

Shen, W.W., Frieden, M., and Demaurex, N. (2011). Remodelling of the endoplasmic reticulum during store-operated calcium entry. Biol. Cell *103*, 365–380.

Siklós, L., Engelhardt, J.I., Alexianu, M.E., Gurney, M.E., Siddique, T., and Appel, S.H. (1998). Intracellular calcium parallels motoneuron degeneration in SOD-1 mutant mice. J. Neuropathol. Exp. Neurol. *57*, 571–587.

Taguchi, J., Fujii, A., Fujino, Y., Tsujioka, Y., Takahashi, M., Tsuboi, Y., Wada, I., and Yamada, T. (2000). Different expression of calreticulin and immunoglobulin binding protein in Alzheimer's disease brain. Acta Neuropathol. *100*, 153–160.

Tu, H., Nelson, O., Bezprozvanny, A., Wang, Z., Lee, S.F., Hao, Y.H., Serneels, L., De Strooper, B., Yu, G., and Bezprozvanny, I. (2006). Presenilins form ER Ca2+ leak channels, a function disrupted by familial Alzheimer's disease-linked mutations. Cell *126*, 981–993.

Urushitani, M., Ezzi, S.A., Matsuo, A., Tooyama, I., and Julien, J.P. (2008). The endoplasmic reticulum-Golgi pathway is a target for translocation and aggregation of mutant superoxide dismutase linked to ALS. FASEB J. *22*, 2476–2487.

Valdez, G., Tapia, J.C., Lichtman, J.W., Fox, M.A., and Sanes, J.R. (2012). Shared resistance to aging and ALS in neuromuscular junctions of specific muscles. PLoS ONE *7*, e34640.

Van Den Bosch, L., Van Damme, P., Bogaert, E., and Robberecht, W. (2006). The role of excitotoxicity in the pathogenesis of amyotrophic lateral sclerosis. Biochim. Biophys. Acta *1762*, 1068–1082.

von Lewinski, F., and Keller, B.U. (2005). Ca2+, mitochondria and selective motoneuron vulnerability: implications for ALS. Trends Neurosci. *28*, 494–500.

Vucic, S., Nicholson, G.A., and Kiernan, M.C. (2008). Cortical hyperexcitability may precede the onset of familial amyotrophic lateral sclerosis. Brain *131*, 1540–1550.

Wang, S., and Kaufman, R.J. (2012). The impact of the unfolded protein response on human disease. J. Cell Biol. *197*, 857–867.

Zagoraiou, L., Akay, T., Martin, J.F., Brownstone, R.M., Jessell, T.M., and Miles, G.B. (2009). A cluster of cholinergic premotor interneurons modulates mouse locomotor activity. Neuron *64*, 645–662.

Zhang, S.J., Zou, M., Lu, L., Lau, D., Ditzel, D.A., Delucinge-Vivier, C., Aso, Y., Descombes, P., and Bading, H. (2009). Nuclear calcium signaling controls expression of a large gene pool: identification of a gene program for acquired neuroprotection induced by synaptic activity. PLoS Genet. *5*, e1000604.

Zhang, X., Li, L., Chen, S., Yang, D., Wang, Y., Zhang, X., Wang, Z., and Le, W. (2011). Rapamycin treatment augments motor neuron degeneration in SOD1(G93A) mouse model of amyotrophic lateral sclerosis. Autophagy *7*, 412–425.